Spectrochimica Acta Part B 79–80 (2013) 31–38

Contents lists available at SciVerse ScienceDirect

Spectrochimica Acta Part B

journal homepage: www.elsevier.com/locate/sab

Femtosecond and nanosecond laser induced breakdown spectroscopic studies of NTO, HMX, and RDX

Sreedhar Sunku, Manoj Kumar Gundawar *, Ashwin Kumar Myakalwar, P. Prem Kiran, Surya P. Tewari, S. Venugopal Rao *

Advanced Centre of Research in High Energy Materials (ACRHEM), University of Hyderabad, Hyderabad 500046, India

ARTICLE INFO

Article history:
Received 5 April 2012
Accepted 29 October 2012
Available online 10 November 2012

Keywords:
Laser induced breakdown spectroscopy
Femtosecond
Nanosecond
High energy materials
CN molecular emission

ABSTRACT

We present our results from the laser induced breakdown spectroscopic studies of 5-Nitro-2,4-dihydro-3H-1,2,4-triazol-3-one (NTO), Octahydro-1,3,5,7-tetranitro-1,3,5,7-tetrazocine (HMX), and 1,3,5-Trinitroperhydro-1,3,5-triazine (RDX) investigated using nanosecond and femtosecond pulses. The presence of C, CN peaks in the spectra, signatures of high energy materials, was confirmed and persistence of emissions has been measured. Some of the Nitrogen peaks in fs LIBS spectra were found to be lower in magnitude (after normalization with N 868.60 nm peak) compared to the ns LIBS spectra. The presence of an additional CN peak in the fs spectra was identified for all samples. The ratio of CN peaks (388.28 nm, 387.08 nm, 386.16 nm) to C peak (247.82 nm), recorded with similar fluences, was discovered to be stronger in the fs case. Some of the possible mechanisms ensuing from our studies towards discrimination of such materials are outlined.

1. Introduction

Several laser based techniques have been developed recently to investigate the potential of identifying hazardous and illicit compounds [1–5]. The challenges involved in this endeavour are on-field and remote detection to avoid damage to human lives, exposure to harsh environments, fast detection, and negligible scope for false positives. Among the various methods investigated recently, laser incuded breakdown spectroscopy (LIBS) has been identified as an attractive, versatile technique with encouraging attributes such as stand-off detection capability, prospective trace material detection, process control, and high speed [6–27]. Continuous efforts have resulted in development of man-portable LIBS and standoff detection successfully tested up to 100 m [28,29]. LIBS has been prolifically evaluated in recent times for detection/identification of explosive residues [15–29], chemical and biological materials [30,31], and landmines [32] etc. Ultrashort laser pulses have tremendous potential in designing novel and sensitive systems for LIBS analysis [33,34]. Conventional LIBS uses nanosecond (ns) pulses whereas short pulse LIBS uses typically femtosecond (fs) pulses. The specific advantages include lower ablation threshold, minimal air entrainment, and reduced background Continuum emission, significant attributes required for efficient detection of explosives [35–41]. The LIBS technique has been fairly successful in a variety of applications such as nuclear forensics [42], cultural heritage monitoring [43], identification of bacteria [39–41], etc. to name a few amongst others reported. Although the LIBS technique is simple, the data analysis is quite cumbersome and occasionally the conclusions drawn are ambiguous. There have been numerous approaches to improve the efficiency such as double/dual pulse LIBS [44,45]. That the LIBS data is sensitive to various parameters including the effects of substrate [46], sample temperature [47], wavelength [48], bandwidth [49], polarization [50], input energy [51] etc. renders it imperative for exploring other mechanisms (e.g. understanding the kinetics/dynamics) towards discrimination/classification of these compounds.

Utilization of ultrashort pulses in the field of ablation, micromachining, and material processing has been well established [52,53]. In the field of LIBS, Baudelet et al. [39–41] have demonstrated that concentration profile of trace elements enabled them to successfully discriminate different species of bacteria, unambiguously, using fs pulses. Significantly, they demonstrated that (a) fs plasma had lower temperature compared to ns plasma (b) a specific ablation regime that favors intramolecular bonds emission with respect to atomic emission. A precise kinetic study of molecular band intensities allowed them to distinguish the contribution of native CN bonds released by the sample from Carbon recombination with atmospheric Nitrogen. Though there are few initial reports of LIBS experiments with fs pulses on explosive related materials [35–37], the mandate has been divided over advantages of utilizing ultrashort pulses. Earlier studies have attempted to identify a few markers for distinguishing HEM's using fs LIBS data [35–37]. For example, Dikmelik et al. [36] observed emission from CN and C_2 molecules in the LIBS spectra of TNT recorded with 1 mJ, 150 fs pulses. In comparison with fs LIBS the longer timescale of ns excitation resulted in severe fragmentation and, as a consequence, they observed emission only from the elemental constituents in the case of TNT. In contrast to reported fs LIBS spectra of explosives (especially TNT) De Lucia et al. [37] observed

* Corresponding authors. Tel.: +91 40 23138811; fax: +91 40 23132800.
E-mail addresses: manojsp@uohyd.ernet.in (M.K. Gundawar), svrsp@uohyd.ernet.in (S.V. Rao).

0584-8547/$ – see front matter © 2012 Elsevier B.V. All rights reserved.
http://dx.doi.org/10.1016/j.sab.2012.11.002

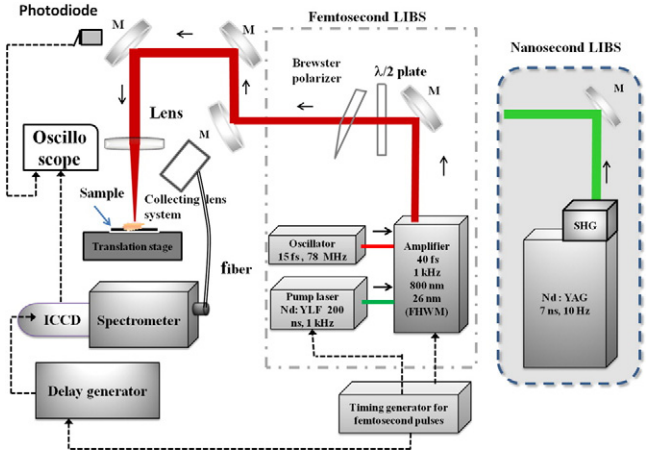

Fig. 1. Schematic of the experimental setup used for ns/fs LIBS.

atomic emission peaks for the constituent elements of explosives — carbon, hydrogen, nitrogen, and oxygen. However, they performed experiments with 10 mJ energy pulses (corresponding to a fluence of 30 J/cm^2). Consequently, futher detailed studies are essential to develop infallible methodologies for the identification/classification of HEMs. Herein, we present some of our experimental results from the LIBS measurements of the commonly used high energy materials such as 5-Nitro-2,4-dihydro-3H-1,2,4-triazol-3-one (NTO), Octahydro-1,3,5,7-tetranitro-1,3,5,7-tetrazocine (HMX), and 1,3,5-Trinitroperhydro-1,3,5-triazine (RDX). The LIBS spectra were collected using a gated ICCD in combination with a spectrometer in ambient atmosphere. The persistence of emission of observed atomic and molecular species were evaluated. Detailed analysis revealed that the CN peak magnitude was observed to be stronger in the fs LIBS data compared to ns LIBS data, obtained at similar fluences. The ramifications of these results towards initial stages of discriminating such materials are discussed.

2. Experimental details

Fig. 1 shows the schematic of experimental set up. Nanosecond pulses at 532 nm (10 Hz, 6 ns FWHM, ~600 mJ), amplified fs pulses at 800 nm (1 kHz, ~40 fs FWHM, ~2.5 mJ) were used for the experiments. The fs amplifier was seeded with ~15 fs pulses (FWHM, spectral bandwidth of 55–60 nm, FWHM) from an oscillator. That the pulses were nearly transform-limited was confirmed using Silhouette (Coherent, USA) measurements (see supplementary information) based on the MIIPS technique [54]. Other specifications include ~6.5 mm (~10 mm) input spot size for ns (fs) pulses and typical energies used were ~20 mJ (~1.6 mJ). The laser pulses were focused (using an 80 mm lens) on the sample mounted on a computer controlled XY translation stage. In fs LIBS experiments the laser pulses had a bandwidth of ~26 nm (FWHM). The samples in both the cases were placed approximately 3–4 mm before the focus (towards the lens) where the spot size was estimated to be ~100 μm. The estimated peak intensity was ~10^{10} W/cm^2 in the ns case where as in the fs case it was ~10^{13} W/cm^2. The calculated fluences were ~250 ± 50 J/cm^2 for the ns pulses and in the range of 30 ± 6 J/cm^2 for the fs pulses. Errors in estimating the fluence arise primarily from evaluation of laser spot size on the sample. Additionally, in order to achieve similar fluences the fs pulses were focused using a 5 cm lens together with slightly higher input energies (2.1 mJ compared to 1.6 mJ in the lower fluence case) providing a fluence of 200 ± 40 J/cm^2. The light was collected by a lens collection system (UV grade fused silica) and the signal was coupled to a fiber and was transferred to an ICCD + spectrometer system (Andor istar DH734 + Mechelle spectrograph), trigger to the ICCD was provided by a delay generator (SRS, DG 532). Since the detector efficiency was not uniform over the entire spectral range we performed appropriate corrections using standard dueterium and halogen lamps before the data was collected. The samples were prepared in the form of a pellet by first grinding the sample with agate mortar and then applying 10 ton hydraulic pressure onto the powdered sample. The obtained pellets were 2–3 mm thick and were placed on an Al sheet/KBr for recording the spectra. The samples were translated using an XY stage so as to expose a new region for the next laser pulse.

3. Results and discussion

Fig. 2(a)–(c) shows typical LIBS spectra recorded from pellets of NTO, RDX, and HMX, respectively, using ns pulses. The data was recorded with a gate width of 1000 ns and a gate delay of 1000 ns with respect to output of the laser pulse. Before 1000 ns (gate delay) we detected strong Continuum in the ns LIBS data. We observed the

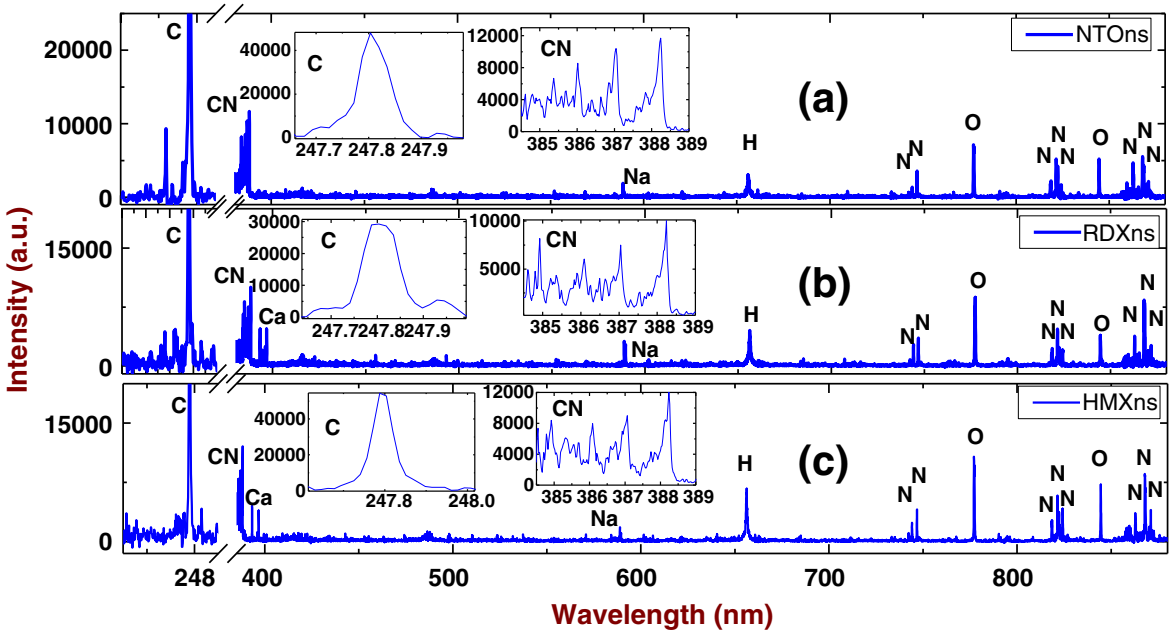

Fig. 2. LIBS spectra of (a) NTO (b) RDX (c) HMX using ns pulses. Gate width of 1000 ns and a gate delay of 1000 ns were used for acquiring the spectra. Each spectrum is resultant of 10 accumulated spectra. Insets show the expanded view of Carbon peak and CN peaks. Fluence used was 250 ± 50 J/cm^2 with samples placed on Al substrate.

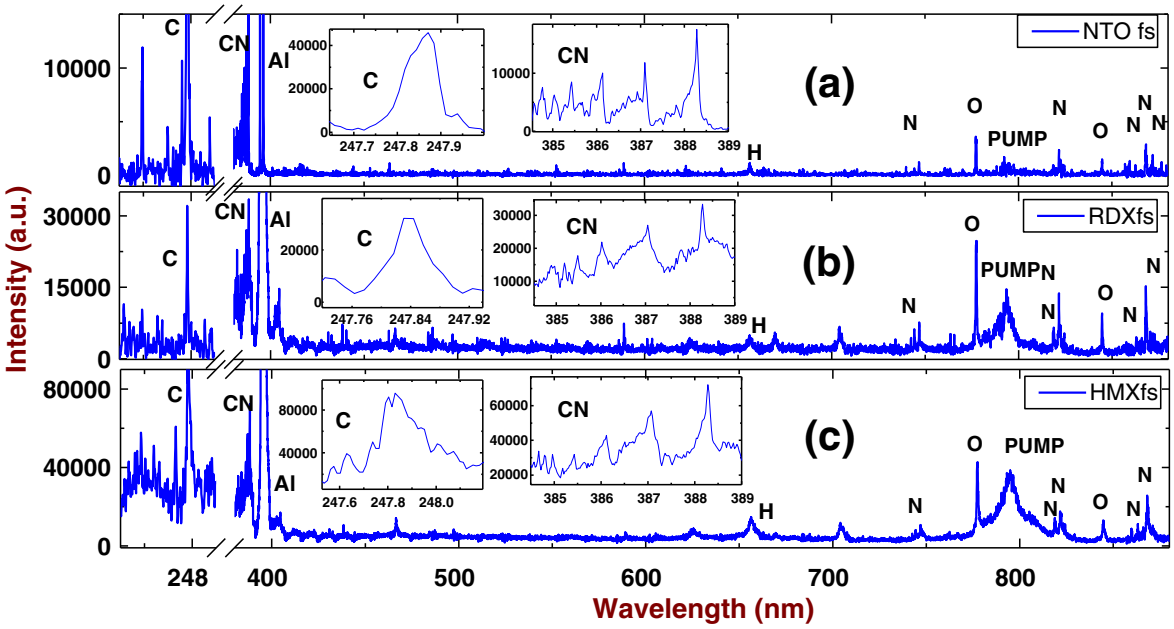

Fig. 3. LIBS spectra of (a) NTO (b) RDX (c) HMX using fs pulses. Gate width used of 300 ns and a gate delay of 100 ns were used for acquiring the spectra. Each spectrum is resultant of 1000 accumulated spectra. Insets show the expanded view of Carbon peak and CN peaks. Fluence used was 30 ± 6 J/cm^2 with samples placed on Al substrate.

peaks of CN, C, H, N, O in all the spectra. Fig. 3(a)–(c) illustrates the LIBS spectra of NTO, RDX, and HMX, respectively, collected using fs pulses. The data was recorded with a gate width of 300 ns and a gate delay of 100 ns. The data was collected after 100 ns delay to avoid contribution from the continuum. We have also observed aluminum peaks in fs LIBS spectra which were confirmed to be from the substrate since the pulses were focused beyond the sample and on to the substrate. The spectra presented in Figs. 2 and 3 are the result of 10 accumulations in the ns case and 1000 accumulations in the fs case. We noticed that the CN peak at 385.01 nm was clearly present in the fs LIBS spectra while the peak was buried within the noise in the ns spectra. Table 1 summarizes the information of all atomic and molecular peaks observed in fs/ns LIBS spectra of all three molecules studied. Some of the Nitrogen peaks observed in fs LIBS spectra were weaker in magnitude compared to ns spectra (for data examined after normalization with the strongest nitrogen peak at 868.60 nm). Typical magnitudes of nitrogen peaks evaluated from the raw data were ~2–9 times the noise in fs case whereas they were ~5–22 times the noise in ns case. Differences in the intensities could, probably, be from differences in plasma temperature between the ns and fs case. The Carbon peak at 247.82 nm was observed in both the cases. CN formation in the fs LIBS case would be aided by C from the sample and N from the sample and/or atmosphere.

To understand the temporal dynamics of LIBS signal [55–57] we had recorded spectra with different gate delays. In case of fs LIBS the spectra were recorded with 50 ns gate width starting at 100 ns with 50 ns interval up to 400 ns (total number of 7 spectra were collected) whereas in ns case the spectra were recorded with 200 ns gate width starting at 100 ns with 200 ns interval up to 3000 ns (total number of 15 spectra were collected). The reason we had taken different series size is that in fs LIBS good signal-to-noise (SNR) ratio was observed up to 400 ns only. In the case of ns LIBS we could achieve good SNR up to 3000 ns for all the samples. The intensity of C, H, N, O, and CN peaks recorded with time delay were fitted with a single exponential decay. Decay constants summarized in Table 2 illustrate that the atomic species have longer life time (of few 100's of ns) with ns pulse excitation whereas for fs excitation their decay time was only few 10's of ns. The error in measurements and fittings was estimated to be ~10% and therefore the values presented in Table 2 are within $\pm 10\%$. The decay time of fs LIBS plasma, in general, is very short compared to ns LIBS plasma. The reason is well established and reported/discussed extensively in literature [58–60]. The interaction mechanism of materials is different for these two pulses and, therefore, the nature of plasma is different. In the fs

Table 1
List of various atomic and molecular peaks in the LIBS spectra of NTO, RDX, and HMX obtained using fs and ns pulses.

Peak	Species	RDX		HMX		NTO	
		ns	fs	ns	fs	ns	fs
247.82	C	*	*	*	*	*	*
279.49, 280.21, 285.10	Mg	*	*	*	*	*	*
385.01	CN	#	*	#	*	#	*
385.40	CN	*	*	*	*	*	*
386.16	CN	*	*	*	*	*	*
387.07	CN	*	*	*	*	*	*
388.28	CN	*	*	*	*	*	*
393.25, 396.77	Ca	*	*	*	*	*	*
394.4, 396.15	Al	*	*	*	*	*	*
588.89, 589.50	Na	*	*	*	*	*	*
656.2	H	*	*	*	*	*	*
742.2, 744.1, 746.8	N	**	*	**	*	**	*
777.20	O (triplet)	*	*	*	*	*	*
818.34, 818.64, 821.50, 822.35,	N	*	*	*	*	*	*
824.22,859.5, 856.74, 862.9, 865.66, 868.03, 870.25, 871.10, 870.74	N	**	*	**	*	**	*
844.55	O	*	*	*	*	*	*
867.80, 868.80	N	*	*	*	*	*	*

* indicates peak present ** indicates higher magnitude # indicates buried in the noise.

Table 2
Summary of the persistence of emission of important atomic and molecular species extracted from the LIBS spectra of RDX, HMX, and NTO acquired using ns and fs pulses.

	Persistence of emission (ns)					
	RDX		HMX		NTO	
Peak-λ(nm)	ns case	fs case	ns case	fs case	ns case	fs case
C-247.82	440	68	480	60	510	52
CN-388.28	703	294	812	92	983	133
H-656.20	370	45	379	47	455	36
O-777.20	354	33	218	20	296	29
O-844.55	295	50	379	50	678	37
N-868.80	353	54	300	37	363	30

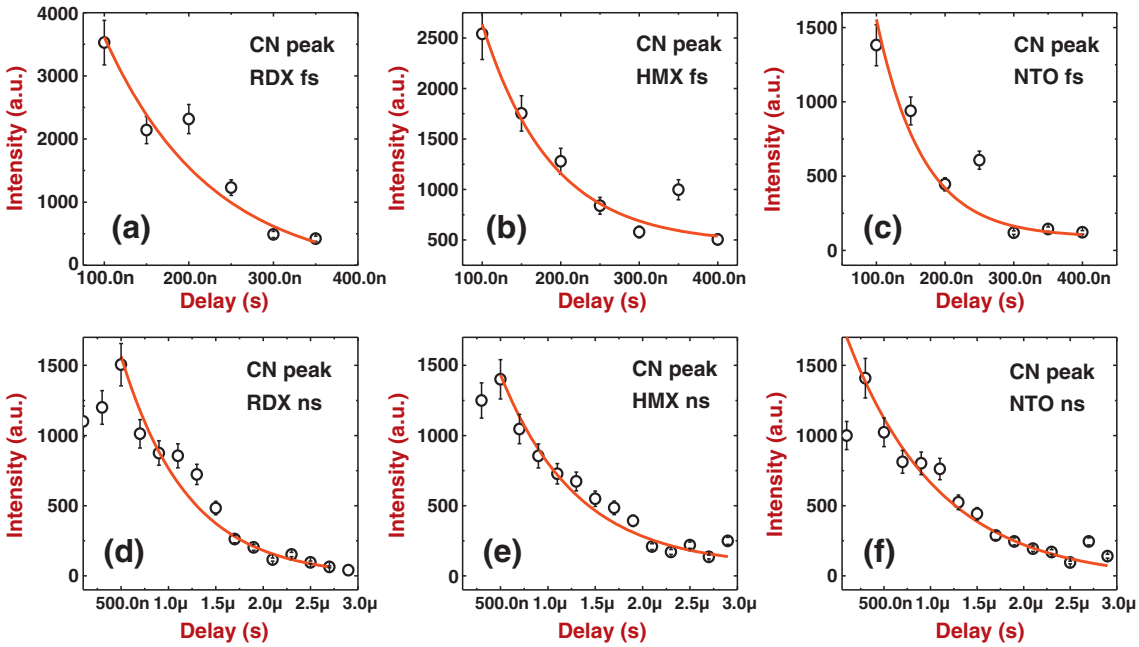

Fig. 4. Time-resolved data of the CN molecular peak (388.28 nm) (a)-(c) fs LIBS data (d)–(f) ns LIBS data recorded with ICCD. 200 ns gate width and an initial gate delay of 100 ns was used for acquiring the spectra and spectra were recorded for every delay of 200 ns up to 2900 ns in the ns case. 50 ns gate width and a starting gate delay of 100 ns was used for acquiring the spectra and spectra were recorded for every delay of 50 ns up to 400 ns in the fs case. Fluence used was 250 ± 50 J/cm^2 in ns case and 30 ± 6 J/cm^2 in fs case.

case, material will be rapidly converted into ionized gas. Because of the short time scales involved, the interaction of fs pulses with plasma is absent after certain time whereas ns pulses interact with several transient states of the plasma. Moreover, in the ns case, pulses interact further with the plasma while plasma re-heating takes place which results in a higher temperature and density of the plasma. This leads to a longer persistence of emission in the case of ns plasmas. Fig. 4(a)–(f) illustrates the decay behavior of CN peak (388.34 nm) for all the samples obtained using fs pulses [(a)–(c)] and ns pulses [(d)–(f)]. A closer inspection of the data in the 1–1.5 μs range suggests a small hump, probably indicating the presence of secondary process. Ma et al. [55] reported their kinetic model of atomic and molecular emission in LIBS studies of organic compounds and demonstrated that four-center reaction $C_2 + N_2 \rightarrow 2CN$ is very unlikely to be the major process during the formation of CN. Rather, the reaction of C and N_2 appeared to be responsible for increased CN concentration at longer delays. Further experiments are required to completely understand this behavior. Fig. 5(a)–(f) illustrates the decay behavior of C peak (247.82 nm) for all the samples obtained using fs pulses [(a)-(c)] and ns pulses [(d)-(f)]. The decay constants are summarized in Table 2. It is evident

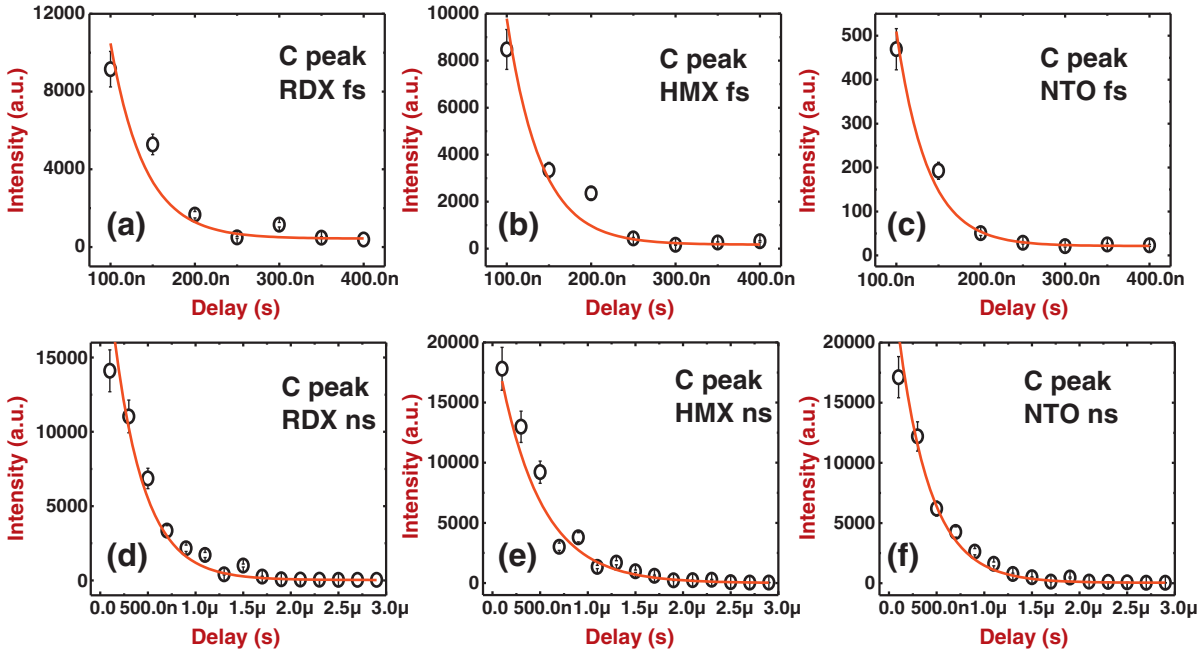

Fig. 5. Time-resolved data of elemental Carbon peak (247.82 nm) (**a**)-(**c**) fs LIBS data (**d**)-(**f**) ns LIBS data recorded with ICCD. 200 ns gate width and an initial gate delay of 100 ns was used for acquiring the spectra and spectra were recorded for every delay of 200 ns up to 2900 ns in the ns case. 50 ns gate width and a gate delay of 100 ns was used for acquiring the spectra and spectra were recorded for every delay of 50 ns up to 400 ns in the fs case. Fluence used was 250 ± 50 J/cm^2 in ns case and 30 ± 6 J/cm^2 in fs case.

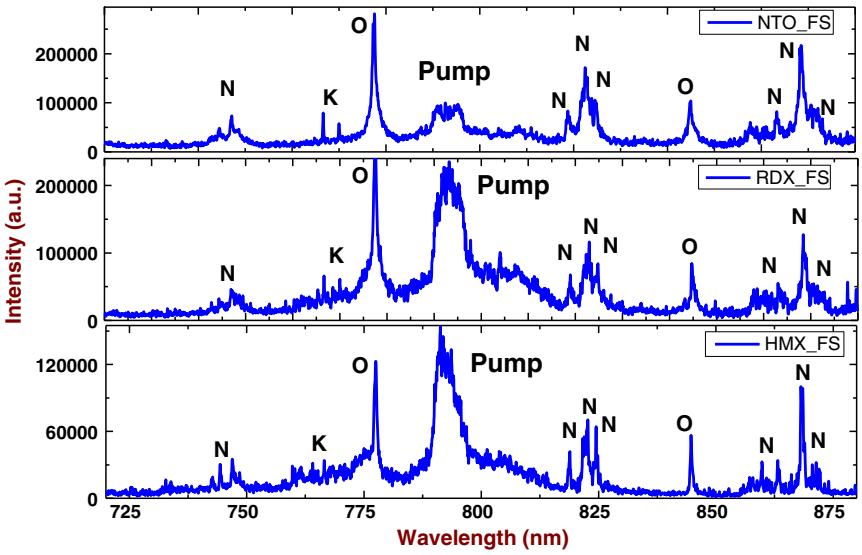

Fig. 6. LIBS spectra of (a) NTO (b) RDX (c) HMX using fs pulses. Gate width used was 800 ns and a gate delay of 100 ns was used for acquiring the spectra. Each spectrum is resultant of 1000 accumulated spectra. Fluence used was 200 ± 40 J/cm^2 with samples placed on KBr substrate.

that the decay was much slower (>400 ns) for the ns C peak compared to the fs C peak (50–70 ns). Further, the decay of CN peak was also slower (~1 μs) with ns pulses compared to fs pulses (<0.3 μs). Intensity of all elemental peaks decayed very fast in fs LIBS spectra compared to ns LIBS spectra.

As previously observed [36,39], our data reveals that under current experimental conditions the behavior of molecular species is different for fs excitation compared to ns excitation. The generation of molecular CN species has been identified to be diverse for different compounds [10,61,62]. Three main routes which possibly could contribute to the formation of molecular CN are (a) direct vaporization of the sample containing CN radicals as intermolecular bonds (b) recombination of the C and N from the compound (c) reaction in the plume containing Carbon (from sample) and Nitrogen (from air) [10]. To compare the ratios of molecular to atomic peaks obtained we had recorded fs spectra with a fluence of 200 ± 40 J/cm^2 and ns spectra with a fluence of 250 ± 50 J/cm^2 for all the HEMs. The data collected with 800 ns gate width and in the spectral range of 700 nm–900 nm is depicted in Fig. 6(a)–(c) for NTO, RDX, and HMX, respectively. Most of the nitrogen peaks were clearly resolved unlike in the low fluence case, depicted in Fig. 3. Fig. 7(a)–(f) shows the plots CN and C peaks in the LIBS spectra observed in all the samples [(a),(b) for NTO, (c),(d) for RDX and (e),(f) for HMX] using both the pulses. The significant observations from our data were (a) the ratios of CN molecular lines (388.28 nm, 387.08 nm, 386.16 nm, 385.438 nm), to C 247.82 nm line, were stronger in the fs LIBS spectra for all three samples. This is evident from the data presented in Fig. 7 where CN/C ratio is lower in the case ns compared to fs case for all the samples. (b) 385.01 nm peak was clearly observed in fs LIBS spectra while in the ns spectra the peak was buried within the noise. The CN/C ratios estimated for all the samples are summarized in Table 3 and include standard deviation and relative standard deviation (%RSD). For the fs spectra we had calculated the ratios with two different fluences (30 ± 6 J/cm^2 and 200 ± 40 J/cm^2). CN/C ratios were estimated for three strongest CN peaks (388.28 nm, 387.08 nm, and 386.16 nm). The intensity calculated was simply the magnitude of peak height with background correction. The CN (388.28 nm)/C (247.82 nm) ratio estimated for NTO with fs pulses (low/high fluences) was $0.28 \pm 0.08/0.37 \pm 0.09$ while for ns pulses it was 0.25 ± 0.04. For the case of RDX the ratios were $0.75 \pm 0.06/1.05 \pm 0.40$ and 0.23 ± 0.05 for fs and ns pulses, respectively. The ratios approximated for HMX were $0.61 \pm 0.13/0.82 \pm 0.35$ and 0.19 ± 0.03 for fs and ns pulses, respectively. The CN/C ratios of ns and fs data of all three CN peaks acquired with similar fluences (and similar gate widths) clearly indicate that the CN formation was indeed superior with fs pulses. The typical signal to noise ratio was >20 in the ns case and >25 in the fs case. Similar trend was observed with LIBS studies on bacteria samples in which they report CN intensity was high in fs LIBS spectra compared to the ns LIBS spectra [39]. These ratios provide useful insight during the discrimination of these compounds. For example, one could look at (a) the presence of C, CN, C_2 peaks (b) CN/C, CN/C_2 and other molecular and atomic ratios as performed successfully by Gottfried et al. [27] (c) the time evolution of CN peak to eliminate Nitrogen based molecules etc.

De Lucia et al. [37] have investigated the efficacy of fs LIBS for detection of explosive residues of RDX, C-4, and Composition-B. They observed a lower threshold for LIBS experiments with ~120 fs pulses in contrast to ns pulses. In RDX spectra they observed stronger C (near 248 nm) emission with fs pulses compared to ns pulses acquired with similar fluences. They have demonstrated that any advantages of fs LIBS over ns LIBS are only likely to be realized at the very low fluences possible with fs pulses. They utilized a gate delay of 50 ns with pulses of 10 mJ energy (corresponding to a fluence of 30 J/cm^2) with a gate width of 5/10 μs and observed Oxygen and Nitrogen emission from atmospheric entrainment in the blank Al spectrum. Our data obtained with ~40 fs pulses and lower fluences (see supplementary information) with pure Al substrates clearly suggested minimal air entrainment. However, the data recorded at higher fluences using fs pulses avoided Al substrate since the samples were placed on a KBr substrate. The samples used were also thicker (~3 mm) to further reduce air entrainment. Most importantly, our pulses have extremely large bandwidth associated with them (~28 nm FWHM corresponding to a total bandwidth of ~65 nm implying that all wavelengths in the 800 ± 32 nm spectral range were available). There is a strong possibility that some of these wavelengths could be resonant with the CN transition (in the spectral range of 384 nm–389 nm) via multi-photon absorption (e.g. 2-photon absorption in this case) thereby inducing slightly larger emission. With the ns pulses the bandwidth involved is extremely small (<1 nm) consequently lacks any resonance. That there was no peaking of the CN intensity with gate delay [63,64] in the fs LIBS data also indicates the contribution is mainly from the constituent C/N or CN of the samples. The plasma chemistry is rather complex in such samples with the possibility of Carbon reacting with Oxygen to form CO (followed by CO_2) and therefore, in the ns case, CN formation could be partially inhibited [56,65,66]. Experiments with exact fluences and devoid of atmospheric intervention are also necessary to absolutely identify the magnitude of

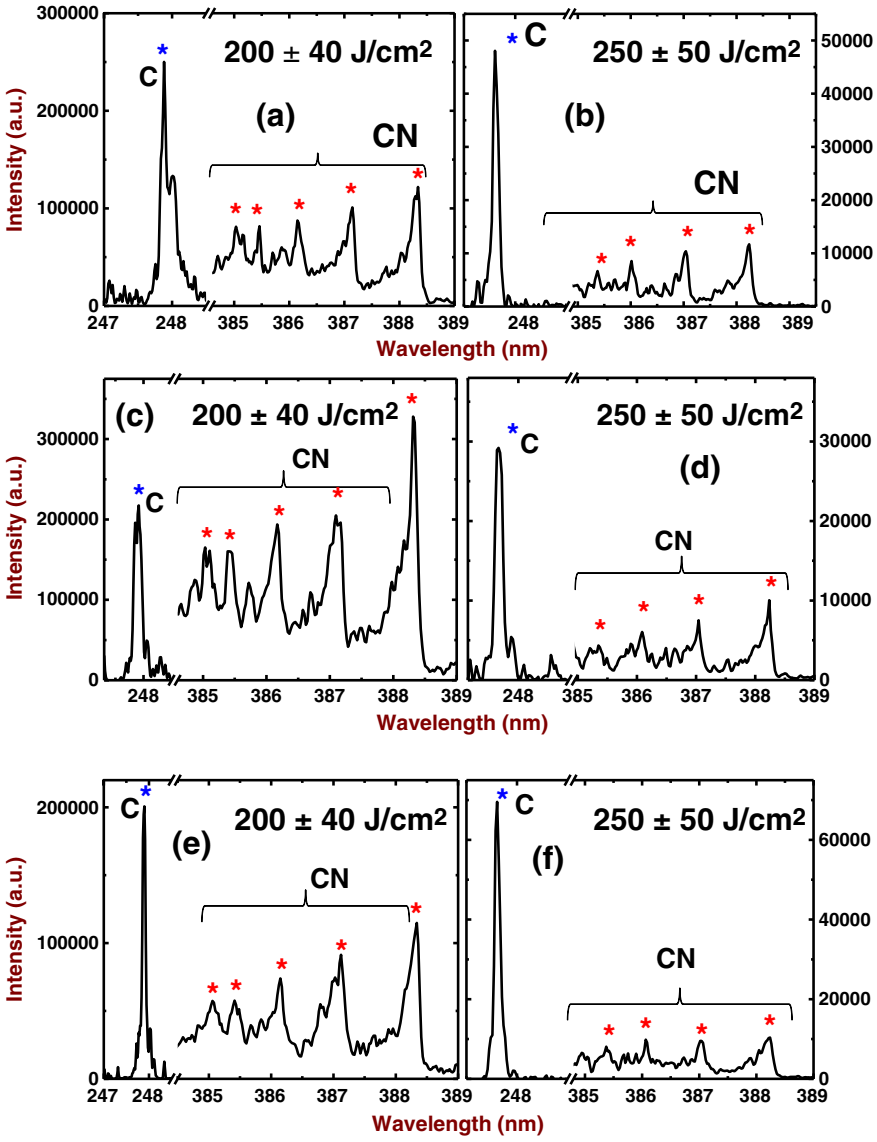

Fig. 7. Comparison of the C and CN peaks obtained in fs, ns LIBS spectra of (a), (b) NTO (c), (d) RDX and (e), (f) HMX. Gate width of 1000 ns and a gate delay of 1000 ns were used for acquiring the ns spectra. Gate width used of 800 ns and a gate delay of 100 ns were used for acquiring the spectra. *'s are guide to peak positions.

CN/C ratios and our efforts are directed towards achieving these. We are in the process of developing appropriate methodologies towards discrimination of HEMs similar to those successfully implemented [67,68]. The present work provides us with an idea of the nature of different pulses (ns/fs) interacting with these materials. Moreover, the behavior of spectral features varying with pulse duration is also understood.

4. Conclusions

We have studied the LIBS spectra of NTO, RDX, and HMX using ns and fs pulses recorded in ambient atmosphere. The elemental and molecular features observed in both spectra were compared. The presence of C and CN peaks in LIBS spectra, signatures for the presence of high energy materials, was confirmed and their persistence

Table 3
CN/C ratios evaluated for NTO, RDX, and HMX for three strongest peaks of CN. The data is an average obtained from 6 independent measurements in each case.

Sample	Ratio	fs − 30 ± 6 J/cm^2	fs − 200 ± 40 J/cm^2	ns − 250 ± 50 J/cm^2
NTO	CN-388.28/C-247.82	0.28 ± 0.08(26.63)	0.37 ± 0.09(24.71)	0.25 ± 0.04 (17.7)
	CN-387.08/C-247.82	0.21 ± 0.06(28.08)	0.28 ± 0.06(22.17)	0.20 ± 0.04 (19.8)
	CN-386.16/C-247.82	0.19 ± 0.04(19.52)	0.22 ± 0.06(25.30)	0.17 ± 0.06(33.41)
RDX	CN-388.28/C-247.82	0.75 ± 0.06(8.15)	1.05 ± 0.40(37.67)	0.23 ± 0.05 (20.2)
	CN-387.08/C-247.82	0.53 ± 0.06(11.20)	0.79 ± 0.28(35.71)	0.20 ± 0.06(29.42)
	CN-386.16/C-247.82	0.37 ± 0.06(16.01)	0.63 ± 0.24(38.42)	0.18 ± 0.10(53.74)
HMX	CN-388.28/C-247.82	0.61 ± 0.13(21.59)	0.82 ± 0.35(45.38)	0.19 ± 0.03(17.76)
	CN-387.08/C-247.82	0.42 ± 0.09(22.41)	0.58 ± 0.24(43.71)	0.15 ± 0.03(19.54)
	CN-386.16/C-247.82	0.25 ± 0.10(40.44)	0.45 ± 0.17(39.81)	0.12 ± 0.03(21.09)

Values are in the format — "Mean ± SD (%RSD)."

of emission has been measured. The persistence of emission of atomic and molecule peaks C, H, N, O, and CN were typically few tens of ns in the fs case and few hundreds of ns in the ns case. One of the CN peaks (at 385.01 nm) was clearly observed in fs LIBS spectra while in the ns spectra the peak was buried within the noise. From the LIBS spectra recorded with similar fluences we observed that the magnitude of CN/C was stronger in the fs case compared to ns case. Further studies in the direction of correlation analysis could provide us a better route for classification of these compounds.

Acknowledgments

We are grateful to the referees for their invaluable comments and suggestions. Financial support from DRDO, India is gratefully acknowledged. The authors also acknowledge the samples provided by HEMRL, Pune, India and P. Ravi, ACRHEM.

Appendix A. Supplementary data

Supplementary data to this article can be found online at http://dx.doi.org/10.1016/j.sab.2012.11.002.

References

[1] L.A. Skvortsov, Laser methods for detecting explosive residues on surfaces of distant objects, Quant. Electron. 42 (2012) 1–11.
[2] M.R. Leahy-Hoppa, J. Miragliotta, R. Osiander, J. Burnett, Y. Dikmelik, C. McEnnis, J.B. Spicer, Ultrafast laser-based spectroscopy and sensing: applications in LIBS, CARS, and THz spectroscopy, Sensors 10 (2010) 4342–4372.
[3] S. Wallin, A. Pettersson, H. Östmark, A. Hobro, Laser-based standoff detection of explosives: a critical review, Anal. Bioanal. Chem. 395 (2009) 259–274.
[4] K. Kim, O.G. Tsay, D.A. Atwood, D.G. Churchill, Destruction and detection of chemical warfare agents, Chem. Rev. 111 (2011) 5345–5403.
[5] J. Moros, J.A. Lorenzo, J.J. Laserna, Standoff detection of explosives: critical comparison for ensuing options on Raman spectroscopy–LIBS sensor fusion, Anal. Bioanal. Chem. 440 (2011) 3353–3365.
[6] In: A.W. Miziolek, V. Palleschi, I. Schechter (Eds.), Laser-Induced Breakdown Spectroscopy (LIBS): Fundamentals and Applications, Cambridge U. Press, 2006.
[7] D.A. Cremers, L.J. Radziemski, Handbook of Laser-Induced Breakdown Spectroscopy, Wiley, 2006.
[8] In: J.P. Singh, S.N. Thakur (Eds.), Laser-Induced Breakdown Spectroscopy, Elsevier, 2007.
[9] D.A. Rusak, B.C. Castle, B.W. Smith, J.D. Winefordner, Fundamentals and applications of laser induced breakdown spectroscopy, Crit. Rev. Anal. Chem. 27 (1997) 257–290.
[10] P. Lucena, A. Doña, L.M. Tobaria, J.J. Laserna, New challenges and insights in the detection and spectral identification of organic explosives by laser induced breakdown spectroscopy, Spectrochim. Acta Part B 66 (2011) 12–20.
[11] D.W. Hahn, N. Omenetto, Laser-induced breakdown spectroscopy (LIBS), Part I: Review of basic diagnostics and plasma particle interactions: Still-challenging issues within the analytical plasma community, Appl. Spectrosc. 64 (2010) 335A–366A.
[12] D.W. Hahn, N. Omenetto, Laser-Induced Breakdown Spectroscopy (LIBS), Part II: Review of Instrumental and Methodological Approaches to Material Analysis and Applications to Different Fields, Appl. Spectrosc. 66 (2012) 347–419.
[13] R. Noll, V. Sturm, Ü. Aydin, D. Eilers, C. Gehlen, M. Höhne, A. Lamott, J. Makowe, J. Vrenegor, Laser-induced breakdown spectroscopy—from research to industry, new frontiers for process control, Spectrochim. Acta Part B 63 (2008) 1159–1166.
[14] F.C. De Lucia Jr., J.L. Gottfried, Rapid analysis of energetic and geo-materials using LIBS, Mater. Today 14 (2011) 274–281.
[15] J.L. Gottfried, F.C. De Lucia Jr., C.A. Munson, A.W. Miziolek, Laser-induced breakdown spectroscopy for detection of explosives residues: a review of recent advances, challenges, and future prospects, Anal. Bioanal. Chem. 395 (2009) 283–300.
[16] M. Abdelhamid, F.J. Fortes, M.A. Harith, J.J. Laserna, Analysis of explosive residues in human fingerprints using optical catapulting–laser-induced breakdown spectroscopy, J. Anal. At. Spectrom. 26 (2011) 1445–1450.
[17] F.C. DeLucia Jr., A.C. Samuels, R.S. Harmon, R.A. Walters, K.L. McNesby, A. LaPointe, R.J. Winkel Jr., A.W. Miziolek, Laser-induced breakdown spectroscopy (LIBS): a promising versatile chemical sensor technology for hazardous material detection, IEEE Sens. J. 5 (2005) 681–689.
[18] R. González, P. Lucena, L.M. Tobaria, J.J. Laserna, Standoff LIBS detection of explosive residues behind a barrier, J. Anal. At. Spectrom. 24 (2009) 1123–1126.
[19] J. Moros, J.A. Lorenzo, P. Lucena, L.M. Tobaria, J.J. Laserna, Simultaneous Raman Spectroscopy—Laser-Induced Breakdown Spectroscopy for instant standoff analysis of explosives using a mobile integrated sensor platform, Anal. Chem. 82 (2010) 1389–1400.
[20] F.C. De Lucia Jr., J.L. Gottfried, C.A. Munson, A.W. Miziolek, Multivariate analysis of standoff laser-induced breakdown spectroscopy spectra for classification of explosive-containing residues, Appl. Opt. 47 (2008) G112–G122.
[21] V. Lazic, A. Palucci, S. Jovicevic, M. Carpanese, Detection of explosives in traces by laser induced breakdown spectroscopy: differences from organic interferents and conditions for a correct classification, Spectrochim. Acta Part B 66 (2011) 644–655.
[22] V. Lazic, A. Palucci, S. Jovicevic, C. Poggi, E. Buono, Analysis of explosive and other organic residues by laser induced breakdown spectroscopy, Spectrochim. Acta Part B 64 (2009) 1028–1039.
[23] F.C. De Lucia, J.L. Gottfried, Classification of explosive residues on organic substrates using laser induced breakdown spectroscopy, Appl. Opt. 51 (2012) B83–B92.
[24] S. Rai, A.K. Rai, S.N. Thakur, Identification of nitro-compounds using LIBS, Appl. Phys. B 91 (2008) 645–650.
[25] F.C. De Lucia Jr., J.L. Gottfried, Characterization of a series of nitrogen-rich molecules using laser induced breakdown spectroscopy, Propellants Explos. Pyrotech. 35 (2010) 268–277.
[26] F.C. De Lucia Jr., R.S. Harmon, K.L. McNesby, R.J. Winkel Jr., A.W. Miziolek, Laser-induced breakdown spectroscopy analysis of energetic materials, Appl. Opt. 42 (2003) 6148–6152.
[27] J.L. Gottfried, F.C. De Lucia Jr., C.A. Munson, A.W. Miziolek, Strategies for residue explosives detection using laser-induced breakdown spectroscopy, J. Anal. At. Spectrom. 23 (2008) 205–216.
[28] C. López-Moreno, S. Palanco, J.J. Laserna, F.C. DeLucia Jr., A.W. Miziolek, J. Rose, R.A. Walters, A.I. Whitehouse, Test of a stand-off laser-induced breakdown spectroscopy sensor for the detection of explosive residues on solid surfaces, J. Anal. At. Spectrom. 21 (2006) 55–60.
[29] J.L. Gottfried, F.C. De Lucia Jr., C.A. Munson, A.W. Miziolek, Standoff detection of chemical and biological threats using laser-induced breakdown spectroscopy, Appl. Spectrosc. 62 (2008) 353–363.
[30] J.L. Gottfried, Discrimination of biological and chemical threat simulants in residue mixtures on multiple substrates, Anal. Bioanal. Chem. 400 (2011) 3289–3301.
[31] J. Diedrich, S.J. Rehse, S. Palchaudhuri, Discrimination of microbiological samples using femtosecond laser-induced breakdown spectroscopy, Appl. Phys. Lett. 90 (2007) 163903.
[32] W. Schade, C. Bohling, K. Hohmann, D. Scheel, Laser-induced plasma spectroscopy for mine detection and verification, Laser Part. Beams 24 (2006) 241–247.
[33] E.L. Gurevich, R. Hergenroeder, Femtosecond laser-induced breakdown spectroscopy: physics, applications, and perspectives, Appl. Spectrosc. 61 (2007) 233A–242A.
[34] P. Rohwetter, J. Yu, G. Mejean, K. Stelmaszczyk, E. Salmon, J. Kasparian, J.-P. Wolf, L. Woeste, Remote LIBS with ultrashort pulses: characteristics in picosecond and femtosecond regimes, J. Anal. At. Spectrom. 19 (2004) 437–444.
[35] Y. Dikmelik, C. McEnnis, J.B. Spicer, Femtosecond laser-induced breakdown spectroscopy of explosives, Proc. SPIE 6217II (2006) 62172A.
[36] Y. Dikmelik, C. McEnnis, J.B. Spicer, Femtosecond and nanosecond laser-induced breakdown spectroscopy of trinitrotoluene, Opt. Express 16 (2008) 5332–5337.
[37] F.C. De Lucia Jr., J.L. Gottfried, A.W. Miziolek, Femtosecond laser-induced breakdown spectroscopy of explosives and explosive-related compounds, Opt. Express 17 (2009) 419–425.
[38] S. Venugopal Rao, S. Sreedhar, M.A. Kumar, P. Prem Kiran, Surya P. Tewari, G. Manoj Kumar, Laser induced breakdown spectroscopy of high energy materials using nanosecond, picosecond, and femtosecond pulses: Challenges and opportunities, Proc. SPIE 8173 (2011) 81731A.
[39] M. Baudelet, L. Guyon, J. Yu, J.-P. Wolf, T. Amodeo, W. Frejafon, P. Laloi, Femtosecond time-resolved laser-induced breakdown spectroscopy for detection and identification of bacteria: a comparison to the nanosecond regime, J. Appl. Phys. 99 (2006) 84701.
[40] M. Baudelet, L. Guyon, J. Yu, J.-P. Wolf, T. Amodeo, E. Frejafon, P. Laloi, Spectral signature of native CN bonds for bacterium detection and identification using femtosecond laser-induced breakdown spectroscopy, Appl. Phys. Lett. 88 (2006) 063901.
[41] M. Baudelet, J. Yu, M. Bossu, J. Jovelet, J.-P. Wolf, T. Amodeo, E. Frejafon, P. Laloi, Discrimination of microbiological samples using femtosecond laser-induced breakdown spectroscopy, Appl. Phys. Lett. 89 (2006) 163903.
[42] F.R. Doucet, G. Lithgow, R. Kosierb, P. Bouchard, M. Sabsabi, Determination of isotope ratios using Laser-Induced Breakdown Spectroscopy in ambient air at atmospheric pressure for nuclear forensics, J. Anal. At. Spectrom. 26 (2011) 536–541.
[43] S. Tzortzakis, D. Anglos, D. Gray, Ultraviolet laser filaments for remote laser-induced breakdown spectroscopy (LIBS) analysis: applications in cultural heritage monitoring, Opt. Lett. 31 (2006) 1139–1142.
[44] F.C. De Lucia Jr., J.L. Gottfried, C.A. Munson, A.W. Miziolek, Double pulse laser-induced breakdown spectroscopy of explosives: initial study towards improved discrimination, Spectrochim. Acta Part B 62 (1997) 1399–1404.
[45] J.L. Gottfried, F.C. De Lucia Jr., C.A. Munson, A.W. Miziolek, Double-pulse standoff laser-induced breakdown spectroscopy for versatile hazardous materials detection, Spectrochim. Acta Part B 62 (2007) 1405–1411.
[46] C. McEnnis, J.B. Spicer, Substrate-related effects on molecular and atomic emission in LIBS of explosives, Proc. SPIE 6953 (2008) 695309.
[47] J. Scaffidi, W. Pearman, J.C. Carter, B.W. Colston, S.M. Angel, Effects of sample temperature in femtosecond single-pulse laser-induced breakdown spectroscopy, Appl. Opt. 43 (2004) 2786–2791.
[48] D.M. Wong, P.J. Dagdigian, Comparison of laser-induced breakdown spectra of organic compounds with irradiation at 1.5 and 1.064 μm, Appl. Opt. 47 (2008) G149–G157.
[49] T. Gunaratne, M. Kangas, S. Singh, A. Gross, M. Dantus, Influence of bandwidth and phase shaping on laser induced breakdown spectroscopy with ultrashort laser pulses, Chem. Phys. Lett. 423 (2006) 197–201.
[50] Y. Liu, J.S. Penczak, R.J. Gordon, Nanosecond polarization-resolved laser-induced breakdown spectroscopy, Opt. Lett. 35 (2010) 112–114.

[51] K.L. Eland, D.N. Stratis, D.M. Gold, S.R. Goode, S.M. Angel, Energy dependence of emission intensity and temperature in a LIBS plasma using femtosecond excitation, Appl. Spectrosc. 55 (2001) 286–291.
[52] B.N. Chichkov, C. Momma, S. Nolte, Femtosecond, picosecond and nanosecond laser ablation of solids, Appl. Phys. A 63 (1996) 134–142.
[53] X. Liu, D. Du, G. Mourou, Laser ablation and micromachining with ultrashort laser pulses, IEEE J. Quantum Electron. 33 (1997) 1706–1716.
[54] B. Xu, J.M. Gunn, J.M. Dela Cruz, V.V. Lozovoy, M. Dantus, Quantitative investigation of the multiphoton intrapulse interference phase scan method for simultaneous phase measurement and compensation of femtosecond laser pulses, J. Opt. Soc. Am. B 23 (2006) 750–759.
[55] Q. Ma, P.J. Dagdigian, Kinetic model of atomic and molecular emissions in laser-induced breakdown spectroscopy of organic compounds, Anal. Bioanal. Chem. 400 (2011) 3193–3205.
[56] P.J. Dagdigian, A. Khachatrian, V.I. Babushok, Kinetic model of C/H/N/O emissions in laser-induced breakdown spectroscopy of organic compounds, Appl. Opt. 49 (2010) C58–C66.
[57] V.I. Babushok, F.C. DeLucia Jr., P.J. Dagdigian, J.L. Gottfried, C.A. Munson, M.J. Nusca, A.W. Miziolek, Kinetic modeling study of the laser-induced plasma plume of cyclotrimethylenetrinitramine (RDX), Spectrochim. Acta Part B 62 (2007) 1321–1328.
[58] V. Margetic, A. Pakulev, A. Stockhaus, M. Bolshov, K. Niemax, R. Hergenr¨oder, A comparison of nanosecond and femtosecond laser-induced plasma spectroscopy of brass samples, Spectrochim. Acta Part B 55 (2000) 1771–1785.
[59] B. Le Drogoff, J. Margot, M. Chaker, M. Sabsabi, O. Barth´elemy, T.W. Johnston, S. Laville, F. Vidal, Y. von Kaenel, Temporal characterization of femtosecond laser pulses induced plasma for spectrochemical analysis of aluminum alloys, Spectrochim. Acta Part B 56 (2001) 987–1002.
[60] J.-B. Sirven, B. Bousquet, L. Canioni, L. Sarger, Time-resolved and time-integrated single-shot laser-induced plasma experiments using nanosecond and femtosecond laser pulses, Spectrochim. Acta Part B 59 (2004) 1033–1039.
[61] K. Sovova, K. Dryahina, P. Spane˘l, M. Kyncl, S. Civis, A study of the composition of the products of laser-induced breakdown of hexogen, octogen, pentrite and trinitrotoluene using selected ion flow tube mass spectrometry and UV–vis spectrometry, Analyst 135 (2010) 1106–1114.
[62] M. Dong, J. Lu, S. Yao, Z. Zhong, J. Li, J. Li, W. Lu, Experimental study on the characteristics of molecular emission spectroscopy for the analysis of solid materials containing C and N, Opt. Express 19 (2011) 17021–17029.
[63] M. Weidman, M. Baudelet, M. Fisher, C. Bridge, C. Brown, M. Sigman, P.J. Dagdigian, M. Richardson, Molecular signal as a signature for detection of energetic materials in filament-induced breakdown spectroscopy, Proc. SPIE 7304 (2009) 73041G.
[64] I. Monch, R. Sattmann, R. Noll, High-speed identification of polymers by laser-induced breakdown spectroscopy, Proc. SPIE 3100 (1997) 64–74.
[65] J.L. Gottfried, Laser-induced plasma chemistry of the explosive RDX with various metallic nanoparticles, Appl. Opt. 51 (2012) B13–B21.
[66] J.B. Simeonsson, A.W. Miziolek, Spectroscopic studies of laser-produced plasmas formed in CO and CO_2 using 193, 266, 355, 532, and 1064 nm laser radiation, Appl. Phys. B 59 (1994) 1–9.
[67] M. Ashwin Kumar, S. Sreedhar, S. Venugopal Rao, P. Prem Kiran, Surya P. Tewari, G. Manoj Kumar, Laser-induced breakdown spectroscopy-based investigation and classification of pharmaceutical tablets using multivariate chemometric analysis, Talanta 87 (2011) 53–59.
[68] N.C. Dingari, I. Barman, M. Ashwin Kumar, Surya P. Tewari, G. Manoj Kumar, Incorporation of Support Vector Machines in the LIBS Toolbox for Sensitive and Robust Classification Amidst Unexpected Sample and System Variability, Anal. Chem. 84 (2012) 2686–2694.